DOI: 10.24874/ti.1899.02.25.07

Tribology in Industry

www.tribology.rs

REVIEW

Prediction of Tribological Behaviour of 3D Printed PLA Using Artificial Neural Network

S.H. Adarsh[a], M. Nagamadhu[b,*], G. Swaminathan[c]

[a]*Department of Mechanical Engineering, Siddaganga Institute of Technology, Tumkur, Karnataka, India,*
[b]*Department of Mechanical Engineering, BMS Institute of Technology and Management, Bangalore, Karnataka, India,*
[c]*Department of Mechanical Engineering, PSG Institute of Technology and Applied Research, Neelambur, Coimbatore, India.*

Keywords:

Tribological Behaviour
Artificial Neural Network
3D printing
Polylactic acid

Corresponding author:

M. Nagamadhu
E-mail: nagamadhu74@gmail.com

Received: 14 February 2026
Revised: 25 March 2026
Accepted: 4 May 2026

A B S T R A C T

This study investigates the influence of 3D printing parameters on the tribological behavior of Polylactic Acid (PLA) specimens under dry sliding conditions. PLA specimens were 3D printed with varying Nozzle Temperatures (200, 210, 220°C), Layer Heights (0.15, 0.18, 0.21mm), Bed Temperatures (70, 75, 80°C), and Infill Density (50, 70, 90%). The specimens were subjected to wear testing using a pin-on-disc setup to evaluate wear, coefficient of friction, frictional force, and pin temperature over the time. An Artificial Neural Network (ANN) with a 5-10-4 architecture was employed, where five input parameters, such as Layer Height (LH), Infill Density (ID), Printing Speed (PS), Nozzle Temperature (NT)) were used to predict four output parameters (wear, coefficient of friction, frictional force, and pin temperature). The ANN model achieved a high correlation coefficient of 0.9838 compared to the experimental results. To further investigate the wear behavior, hardness testing and Scanning Electron Microscopy (SEM) were performed. The results showed that the sample with NT: 200°C, LH: 0.15mm, BT: 70°C, ID: 50% exhibited minimal wear, while the sample with NT: 220°C, LH: 0.18mm, BT: 70°C, ID: 90% showed the maximum wear. These findings highlighted the critical role of 3D printing parameters in optimizing the tribological performance of PLA materials for various applications.

© 2026 Published by Faculty of Engineering

Article in Press

1. INTRODUCTION

In recent days, Polylactic Acid (PLA) has garnered significant attention for its use in tribological wear applications, particularly in scenarios where biodegradable materials and low friction are required. PLA's inherent properties make it suitable for the applications commonly used in medical devices, low-speed sliding components, and biodegradable packaging. However, due to its relatively low melting point, PLA has limited applications in high-speed or high-temperature tribological applications [1-3]. The tribological behavior of 3D-printed PLA specimens, specifically with wear, friction, and lubrication has gained increasing interest among material science

researchers. Although, PLA being widely used in 3D printing due to its ease of fabrication, biodegradability, and relatively low cost [4,5], its tribological properties, such as wear resistance and frictional characteristics are pivotal in determining its performance in dynamic systems involving sliding contacts and relatively moving parts. It has been noticed that PLA exhibits relatively high friction compared to other 3D printing materials like nylon or PTFE (polytetrafluoroethylene), which results in excessive heat generation and wear under sliding conditions. Furthermore, it has a limited wear resistance. Under high mechanical stress and frictional conditions, PLA tends to degrade drastically, making it less suitable for high-performance tribological applications unless its properties are modified with specific additives [6].

Previous research works have revealed several factors that influence the tribological performance of 3D-printed PLA part, including the density of the infill structure, color, layer orientation, and the incorporation of reinforcement materials [7-11]. Higher the infill densities, such as 100% solid configurations, improve wear resistance and reduce friction. The orientation of the printed layers also plays a critical role in mechanical performance, where parts printed with layers aligned along the direction of motion exhibiting superior tribological behavior compared to those with layers oriented perpendicular to the motion. Other factors such as printing temperature, surface finish, and post-processing methods also affect the PLA's tribological performance. Higher printing temperatures can enhance surface smoothness, leading to reduced friction, although this can increase the risk of deformation under load. Subsequently, smoother surfaces, achieved through higher-resolution printing or post-processing, lead to lower friction and improved wear resistance, while rough surfaces tend to accelerate wear due to increased contact area and roughness [12-13].

Despite its limitations, PLA is well-suited for low-stress tribological applications such as no-load-bearing components, prototypes, and aesthetic parts. However, for high stress tribological applications, modifications to the material or processing methods are required to improve the tribological properties. Several studies have investigated various aspects of PLA's mechanical and tribological properties. Shivasharanappa et al. explored the role of modeling in predicting wear data and emphasizing the importance of accurate predictions in tribological performance [14]. Funsho et al. applied the statistical regression model by using Analysis of Variance (ANOVA) to predict wear behavior and found it suitable for forecasting tribological performance [15]. Grasso et al. examined the relationship between Young's modulus, ultimate tensile strength, strain at failure, and stress at failure, thereby noticed a strong correlation between stiffness and strength with infill orientation and temperature settings [16]. Shady et al. focused on enhancing the properties of PLA through plasticizer blending, adding nucleation agent, and nano-formulations, which has shown significant improvements in the material properties [17]. Perepelkina et al. investigated the friction coefficients of various polymers, correlating them with printing parameters [18].

Anouar et al. studied the effects of varied printing orientations (e.g., [0°, 15°, −15°]) relative to the test bar's long axis on the tensile properties of PLA and PLA-CF composites. They have revealed that annealing has improved the crystallinity and mechanical properties of the test samples. The study also found that lower cooling rates led to higher crystallinity and improved Young's modulus compared to as-printed parts [19]. Behzadnasab et al. examined the influence of printing conditions on mechanical properties, noting that increasing NT from 34 MPa to 56 MPa improved the strain at break value, while the annealing process negatively impacted mechanical properties [20]. Many researchers have extensively studied the mechanical properties of PLA, focusing on the aspects such as tensile strength, modulus, strain at failure, and overall structural integrity under various loading conditions [21-23]. These studies have provided valuable insights into the material's behavior and its potential for a wide range of applications. However, research on the tribological behavior of PLA, which is critical for applications involving wear, friction, and lubrication, remains limited. The tribological properties of PLA—such as its wear resistance and frictional characteristics—play an essential role in determining its performance in dynamic systems where sliding or moving contacts occur. As such, there is a notable gap in the literature regarding the specific influence of processing parameters, material modifications, and additives on the tribological behavior of PLA.

Article in Press

Among the many factors influencing PLA's mechanical and tribological properties, nozzle and extraction temperatures are considered to be highly critical. These processing parameters significantly affect the material properties of the final product, especially when reinforcement agents like carbon fibers, glass fibers, or nanoparticles are incorporated into the PLA matrix. The Nozzle Temperature, which controls the extrusion temperature during 3D printing, thereby directly influencing on the flow characteristics, crystalline structure, density, and adhesion of the layers for the 3D printed material. Similarly, the extraction temperature, which is associated with the post-processing steps like annealing, influences the crystallization rate, polymer chain alignment, and overall material strength [24-30].

The phenomenon of enhancing PLA's mechanical properties, predominantly while applying reinforcement agents has been well established, thus optimizing nozzle and extraction temperatures during 3D printing process has been regarded is highly crucial. These reinforcing agents, which are blended with PLA to improve the strength, stiffness, and wear resistance require specific processing conditions to achieve the desired performance. The interaction between the reinforcement agents and PLA's polymeric matrix is highly dependent on the extrusion temperature, as it affects the dispersion, bonding, and alignment of the reinforcements within the material. A higher Nozzle Temperature can improve the homogeneity of the material, leading to better mechanical properties and more uniform tribological behavior.

It is also noticed that the extraction temperature plays a key role during annealing, one among the post-processing stages of PLA. Annealing improves crystallinity, thereby enhancing the mechanical and tribological properties. Higher annealing temperatures can promote improved crystallinity, which generally results in improved wear resistance and lower friction. However, excessively increasing the temperatures may lead to undesirable effects, such as warping or dimensional instability, especially in the case of 3D-printed components.

Although the mechanical properties of PLA have been well-documented, there remains a significant gap in research focused on its tribological performance, predominantly while considering the effects of different printing conditions and post-processing treatments. While previous studies have explored the mechanical behavior of PLA and partially addressed its tribological characteristics. Limited works have systematically evaluated the interplay between Nozzle Temperature (NT), Layer Height (LH), Bed Temperature (BT) and Infill Density (ID) on wear, coefficient of friction (CoF), frictional force, and thermal response under dry sliding conditions. Moreover, existing research has seldom incorporated both quantitative wear metrics and qualitative surface morphology analysis via SEM to identify wear mechanisms.

It has been noticed in some research works, exploring the tribological behavior. However, very limited work has used the advanced modeling techniques like Artificial Neural Networks to predict wear, friction, and other tribological characteristics of PLA under various conditions. Furthermore, the influence of reinforcement agents, ID, and printing temperature on the tribological properties of PLA is not completely explored.

Therefore, further research is essential to explore the relationship between processing parameters and tribological behavior, as well as to identify methods for improving PLA's wear resistance and frictional properties in more demanding applications. The novelty of the present study lies in its integrated approach, combining experimental wear testing with advanced predictive modeling using Artificial Neural Networks (ANN) to establish robust correlations between key 3D printing parameters and tribological performance metrics of PLA.

The primary objectives of this work are to:

1. Investigate the effect of 3D printing parameters, including NT, LH, BT, and ID, on the tribological behavior of PLA under dry sliding wear conditions.
2. Develop a predictive model using Artificial Neural Networks (ANN) to correlate the input parameters (printing settings) with output tribological properties (wear, coefficient of friction, frictional force, and pin temperature).
3. Analyze the wear behavior of PLA through hardness testing and scanning electron microscopy to identify the optimal printing conditions that minimize wear and friction.

Article in Press

2. MATERIALS AND METHODS

2.1 Materials

In the present work, a commercially available Polylactic acid (PLA) filament made by Polymaker with diameter 1.75 mm is used along with Creality Ender 3 Pro 3D printer for printing the test specimens. Based on the literature it is evident that process parameter during the print has a significant effect on the surface finish and strength of the specimen. Therefore, the specimen samples were prepared with varied process parameters like NT, LH, BT, and ID. Fig. 1 shows the flow chart of the methodology adopted in the present work. The steel disc used was EN31 tool steel, with the following composition: C (1.1%), Mn (0.6%), Cr (1.2%), and Fe (balance). The surface roughness (Ra) of the disc was measured at 0.2 µm, ensuring a smooth and consistent sliding surface.

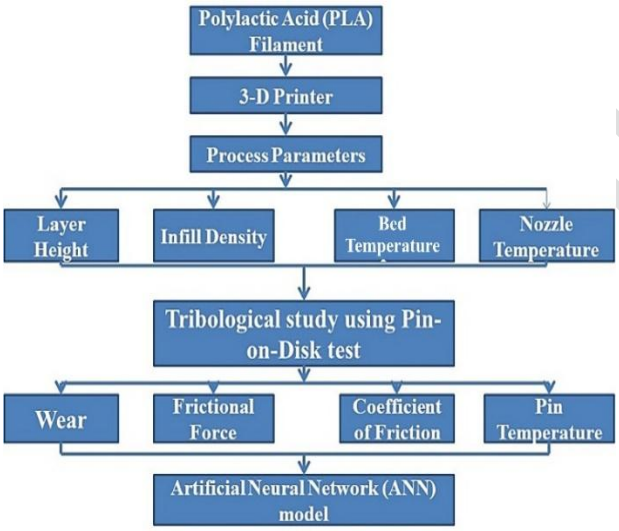

Fig. 1. Methodological Flow chart.

2.2 Processing of Samples

The cylindrical pin has a diameter of 8 mm and a height of 34 mm shown in Fig. 2. The pins are designed in SolidWorks and exported as an STL file. This file is imported into Simplify 3D slicing software. The modified settings were NT, LH, BT, and ID are shown in Table 1. The cylindrical pins are printed horizontally.

All printing parameters were varied for each sample keeping a constant diameter of 1.75 mm for PLA filament with a raster angle of 0°. A constant printing speed of 60 mm/s was maintained throughout the process.

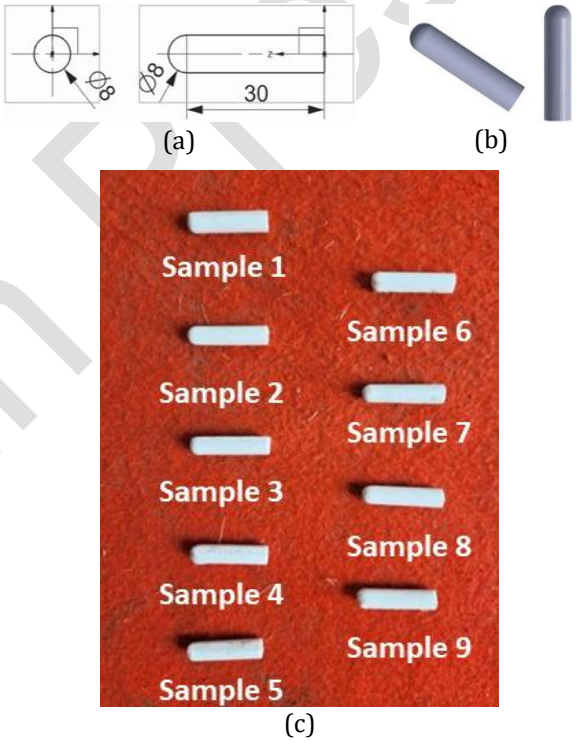

Fig. 2. (a) Sample dimensional details (b) CAD model for 3D printing (c) 3D Printed PLA pin samples to study tribological behavior.

Table 1. Table for 3D printing parameters.

Sl. No.	Nozzle Temperature (NT) in °C	Layer Height (LH) in mm	Bed Temperature (BT) in °C	Infill Density (ID) in %
1	200	0.15	70	50
2	200	0.18	75	70
3	200	0.21	80	90
4	210	0.15	75	90
5	210	0.18	80	50
6	210	0.21	70	70
7	220	0.15	80	70
8	220	0.18	70	90
9	220	0.21	75	50

While printing the wear testing specimens (pins) horizontal orientation was maintained for all the specimens to enhance interlayer bonding strength along with the loading direction during the pin-on-disc test. While printing with horizontal orientation, the layers were made to align perpendicularly to the sliding direction to simulate real-world contact and friction scenarios and also to provide an in-depth understanding of tribological performance under shear loading. Furthermore, horizontally printed specimens reduce the likelihood of delamination of layers during sliding, which is a major concern in vertically printed specimens, where layer lines are parallel to the applied load. This approach was chosen based on previous studies demonstrating improved mechanical integrity and wear resistance in horizontally printed samples.

2.3 Tribological test

A pin-on-disc tribometer is a widely used experimental apparatus designed to study the tribological properties, such as friction, wear, and lubrication, of materials under controlled conditions. which is essential for developing durable and efficient mechanical systems. It plays a crucial role in material science and engineering, helping researchers understand the wear behavior of different materials and coatings, which is essential for developing durable and efficient mechanical systems. All samples were printed using 3 contours / perimeters, 3 top layers, 3 bottom layers, and a rectilinear infill pattern to ensure consistency and reproducibility.

Wear testing carried out with a pin-on-disc tribometer shown in Fig. 3 tested under dry sliding conditions and the test procedures of ASTM G99. The 3D-printed PLA pins were slid against the steel disc at fixed test conditions.
A pin was placed in the pin holder and clamped down to prevent the pin from moving and vibrating strongly in the pin holder. The temperature was measured using an infrared (IR) sensor (accuracy ±0.5°C), positioned 10 mm above the sliding pin surface. Testing parameters are of are shown in Table 2. Measurements were recorded at 5-minute intervals throughout the 45-minute test to monitor temperature changes in real-time without contact.

Fig. 3. Pin-on-Disc Experimental setup.

Table 2. Test Parameters for pin on disc test.

Test Conditions	Value
Rotating disc speed (RPM)	100
Normal load (N)	5
Test duration (min)	45
Lubrication	Dry
Track radius (mm)	60

2.4 Scanning electron microscope

The high-performance Scanning Electron Microscope (SEM) is an advanced analytical instrument designed for precise surface characterization of materials at the micro- and nanoscale. The SEM used in this work offers an exceptional resolution of 3.0 nanometers (nm), enabling detailed imaging of fine surface features, microstructural components, and morphological variations in a wide range of specimens. One of its key features is the ability to operate in Low Vacuum (LV) mode, which allows the examination of non-conductive and wet specimens without the need for extensive sample preparation, such as sputter coating with conductive materials. This is particularly beneficial when analyzing biological samples, polymers, ceramics, or composite materials with insulating phases. The LV mode reduces surface charging and beam damage, thereby preserving the specimen's natural state and providing more accurate observations. The SEM is equipped with an asynchronous five-axis motorized stage, which provides precise movement in the X, Y, Z (vertical), tilt, and rotation axes, allowing for flexible positioning and orientation of the sample under the electron beam.

Article in Press

The stage can accommodate specimens of up to 8 inches (approximately 200 mm) in diameter, making it suitable for both small-scale materials and large industrial components. With an intuitive user interface and advanced imaging software, the SEM is capable to capture high-resolution images, perform elemental analysis (with EDS integration), and conduct failure analysis, microstructural investigations, and topographic mapping. The system's versatility, resolution, and sample handling capabilities make it an invaluable tool in fields such as materials science, metallurgy, semiconductor inspection, nanotechnology, biomedical research, and quality control in manufacturing.

2.5 Artificial neural network

Artificial Neural Networks (ANNs) are a subset of machine learning algorithms that are inspired by the structure and function of the human brain. They are designed to recognize patterns, learn from data, and make decisions based on the information they have processed [31-33]. ANNs are composed of interconnected nodes, or "neurons," which are organized in layers. These layers typically include an input layer, one or more hidden layers, and an output layer [34].

In the present work 5-10-4 ANN architecture is used where 5 refers to the input parameters (NT, LH, BT, ID and testing time), 10 refers to the number of neurons and 4 refers to the output parameters (Wear, Coefficient of friction, Frictional force and Pin temperature) as illustrated in Fig. 4. The basic structure of an ANN consists of three types of layers shown in Fig. 5. and training variables are in Table 3.

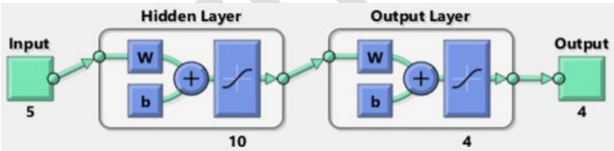

Fig. 4. Neural network connections.

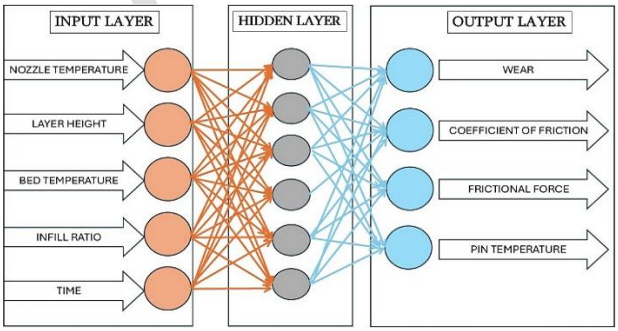

Fig. 5. ANN Architecture.

Table 3. Training variables for the neural network.

Name of Network Parameters	Content
Network	Feed-forward back propagation
Training function	TrainLM
Performance function	Mean Square Error
Adaption learning function	Learngdm
Training epoch	10000
Goal	$1X10^{-6}$
Transfer function of hidden layer	Tan-sigmoid
Transfer function of output	Liner(purelin)
Number of neurons	10

2.6 Hardness testing

The Shore D hardness test, defined by ASTM D2240 and ISO 868, measures the hardness of rigid materials like plastics using a durometer. It determines the depth of indentation under a specific force, with higher Shore D values indicating harder materials. Each sample was tested in five different areas to finalize the hardness value. For 3D-printed PLA, this test is crucial to assess the resistance to indentation, reflecting the material's rigidity and durability. PLA, known for its ease of printing and eco-friendliness, exhibits varying hardness based on print parameters and material formulation. The Shore D scale ranges from 0 to 100 and is widely used to evaluate the mechanical performance of PLA in additive manufacturing applications.

3. RESULTS AND DISCUSSION

Output parameters like, wear, frictional coefficient, frictional force and pin temperature are dependent on various input parameters. However, the testing time also considered for the variance in the output parameters (NT, LH, BT, and ID). The prime goal was to understand the effect of all the input parameters on the mechanic al properties listed as output parameter with respect to testing time. Individual output parameters was plotted against the testing time considering all the samples prepared by 3D printing. Fig. 6 illustrates the variation in wear with respect to testing time for different samples, in which Sample 1 with a NT of 200°C, a LH of 0.15 mm, a BT of 70 °C, and an ID of 50% exhibited lowest wear.

Article in Press

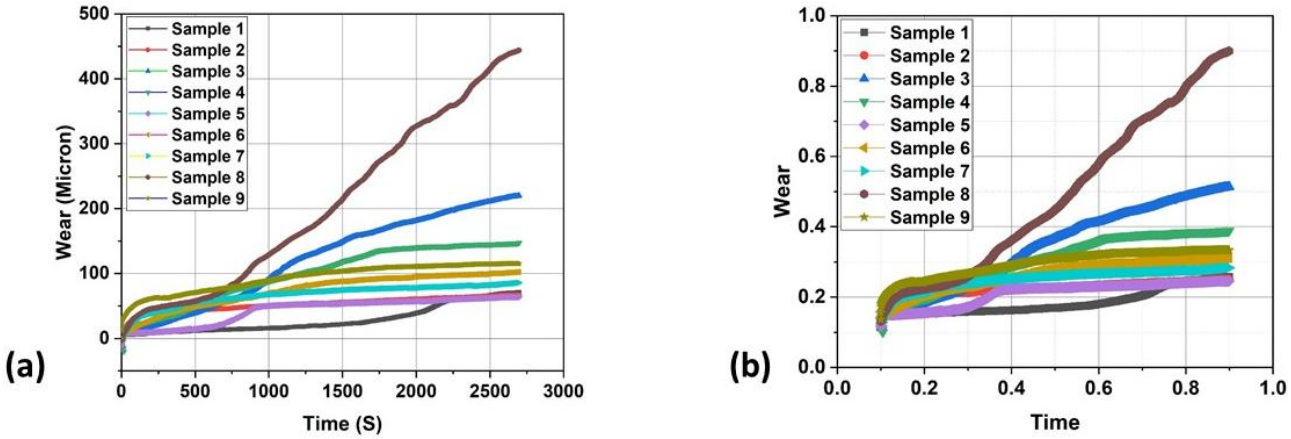

Fig. 6. Wear v/s Time for various samples (a) Actual values (b) Normalized values.

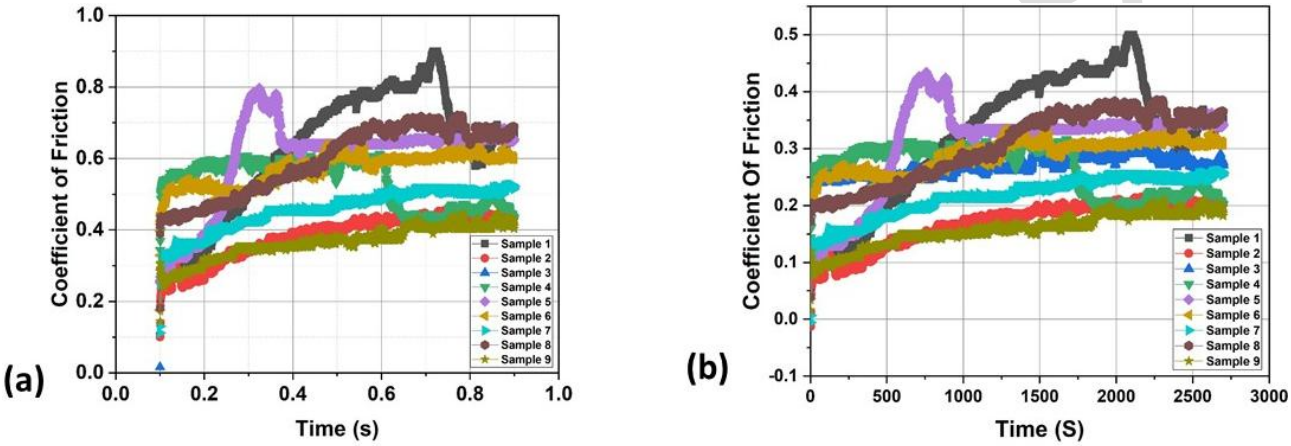

Fig. 7. Coefficient of Friction v/s Time for various samples (a) Actual values (b) Normalized values.

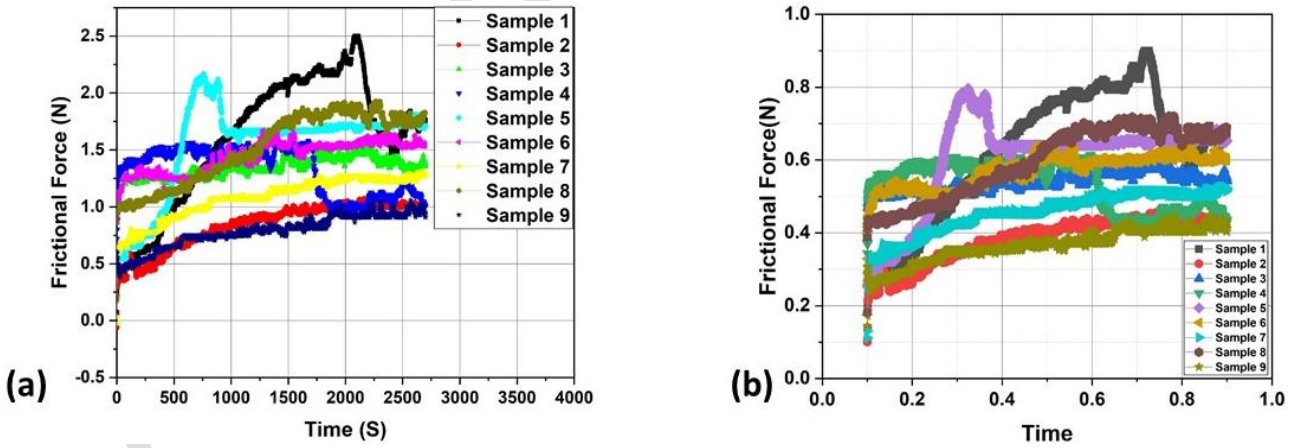

Fig. 8. Frictional Force v/s Time for various samples (a) Actual values (b) Normalized values.

In contrast, Sample 8, with a NT of 220°C, a LH of 0.21 mm, a BT of 75°C, and an ID of 50%, shown the highest wear. This difference in wear behavior is attributed to the hardness values of the samples, with Sample 1 having a lower hardness of 70 Shore D, while Sample 8 has a higher hardness of 75 Shore D. Fig. 7 depicts the variation of the Coefficient of Friction (CoF) with respect to time for the different samples. As expected, the CoF increases over time, indicating that as wear progresses and surface roughness increases, friction between the pin and the surface also escalates. The coefficient of friction varies from 0.1 at the initial stages of testing to 0.5 towards the end. This progression can be linked to changes in the contact surface area, material wear, and the accumulation of heat, which eventually increases the friction between the contacting surfaces. Fig. 8

presents the variation of frictional force as a function of time. Frictional force increases progressively with time, with values ranging from 0.5 N at the start of the test to 2.5 N towards the end. The increase in frictional force with respect to time can be attributed to the continuous degradation of the material's surface, which leads to higher resistance during the sliding contact. Similar results are also found in various research by considering LH, printing temperature, and speed [35-38].

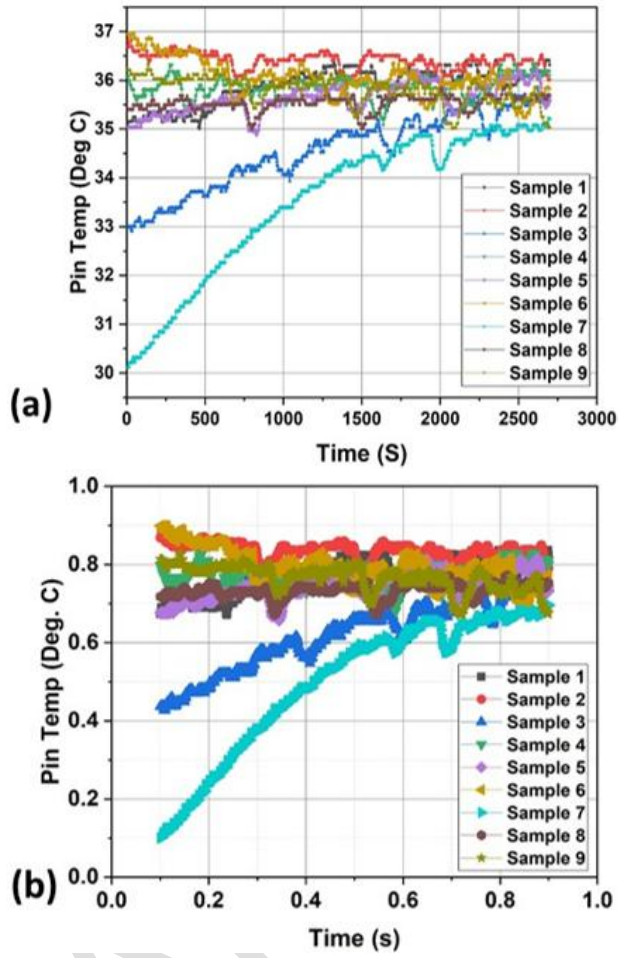

Fig. 9. Pin temperature v/s Time for various samples (a) Actual values (b) Normalized values.

The increase in frictional force is directly correlated with the rise in the coefficient of friction, suggesting that both factors are interrelated and jointly contribute to the wear mechanism. Fig. 9 illustrates the variation of pin temperature over time. As the test progresses, the pin temperature increases steadily, rising from room temperature to approximately 37°C. This temperature increase can be attributed to the heat generated by the frictional interaction between the pin and the material surface. As the frictional force escalates, additional heat is produced, resulting in a corresponding rise in the pin temperature. This thermal effect can potentially influence the material properties of the samples, leading to alterations in the wear behavior as the temperature continues to rise. The increase in temperature may cause changes in the material's mechanical properties, such as hardness or elasticity, which could, in turn, affect the wear rate and overall performance. Similar results are also found in various research works [39-40]. In the context of Artificial Neural Network (ANN) modeling, normalization of the input and output variables is performed within the range of 0 to 1. This is commonly achieved using a specific mathematical equation that standardizes the corresponding data for consistency, ensuring that the values are appropriately scaled for the neural network's processing [41-43]. This normalization helps improve the accuracy and efficiency of the model by preventing any single variable from disproportionately influencing the results due to its scale.

$$X' = 0.1 + 0.8 * \left(\frac{X - X_{Min}}{X_{Max} - X_{Min}}\right) \quad (1)$$

Where: X': Normalized value, X: Original value, X_{Min}: Minimum value of the datasetand, X_{Max}: Maximum value of the dataset.

4. ANN RESULTS

MATLAB based neural network training tool was used for neural network analysis which is as shown in Fig. 10. Similarly, Fig. 11 illustrates the variation of the Mean Squared Error (MSE) with respect to the number of epochs. Although MSE seems to be maximum at initial stages, as the neural network training progresses through multiple iterations, the MSE decreases consistently with each epoch.

This reduction in MSE indicates that the neural network training tool is gradually learning the patterns within the dataset thereby improving its accuracy. As neural network training tool progresses through the training process, the error gets converge towards a minimum level, signifying that the model is approaching an optimal solution and is refining its predictions with every epoch. This iterative process highlights the efficiency of the neural network in minimizing the discrepancy between predicted and actual values.

Article in Press

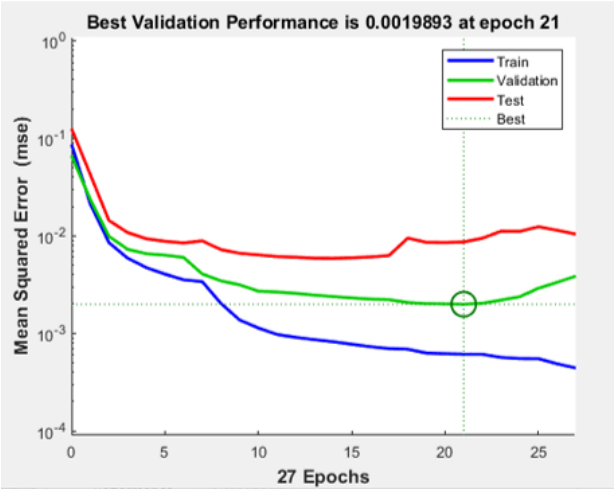

Fig. 10. Artificial Neural Network training in MATLAB software.

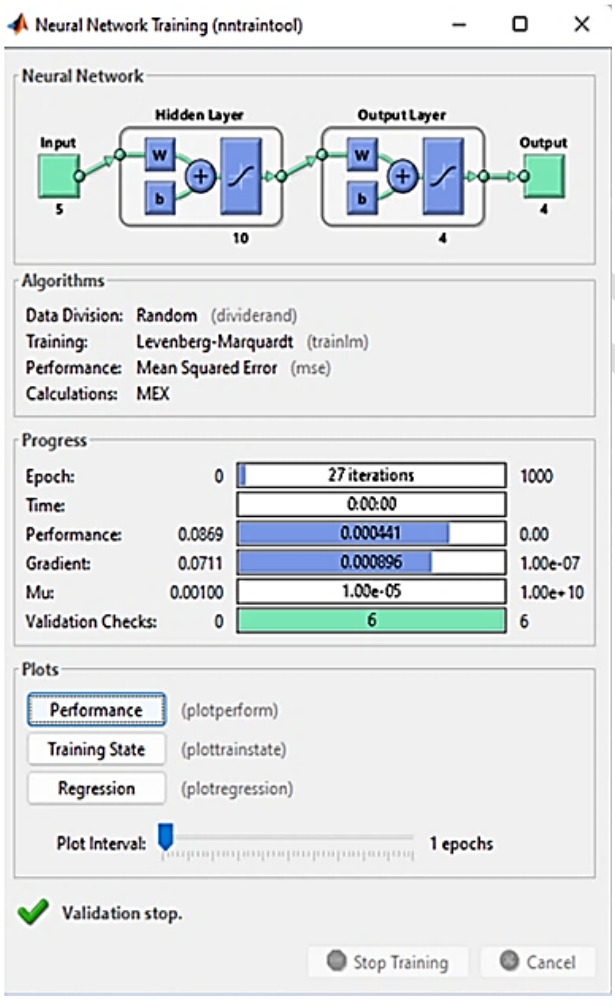

Fig. 11. Performance of the network (Mean square error v/s Epoch).

It can be noticed that throughout the analysis the experimental data is divided into two sections: Training dataset (90%) and Testing dataset (10%). The training dataset is used to train the ANN model while the testing dataset is used to cross-validate the ANN model [41-43].

The correlation coefficient (R) value calculated on training datasets (Training-R) is 0.99507, indicating a very strong positive correlation between the predicted and actual values during the training phase. Since the Training-R value is close to 1, which suggests that the neural network has effectively learned the relationships in the training data, with minimal error and with high accuracy.

All the data were well fitted by the neural network tool, thereby the training error has been substantially minimized. As it is noticed in the decreasing Mean Squared Error (MSE) over epochs discussed earlier.

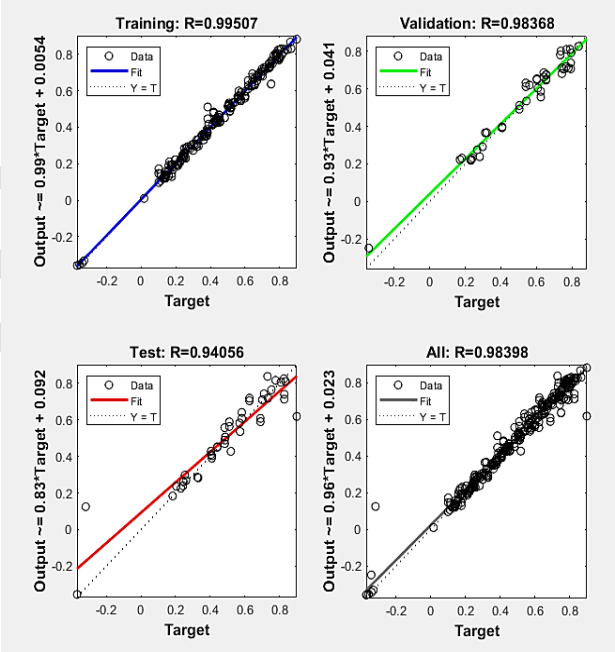

Fig. 12. Correlation coefficient of ANN result.

The correlation coefficient values as shown in Fig. 12 reflects the performance of the Artificial Neural Network (ANN) across different stages of training, validation, testing, and overall performance. The R value under validation is 0.98368, this correlation coefficient represents the relationship between the predicted and actual values during the validation phase. The validation data is used to check how well the network generalizes to new, unseen data. A value of 0.98368 indicates that the model performs very well on validation data, with a high degree of accuracy and minimal overfitting.

The slight drop in the valuation R-value in comparison with the training R-value suggests that the model is still generalizing well but might be slightly more optimized for the training data.

The test R-value is 0.94056, this correlation coefficient measures the accuracy of the model on a completely new dataset that was not used during the training or validation phases. A value of 0.94056 shows that the neural network still performs well on the test data, but there is a more noticeable decrease in correlation compared to the training and validation phases. This drop may indicate that the model is starting to lose some predictive power on data it hasn't seen before. However, the overall correlation remains strong, indicating good generalization. AII R-value is 0.98398, this correlation coefficient represents the overall performance of the model, considering all the phases (training, validation, and testing). With a value of 0.98398, the model suggests that, on average, the model performed consistently well across all datasets.

A slight decrease from the training phase is expected, but overall, the model has demonstrated strong generalization and high accuracy. Fig. 12, 13, and 14 shows the accuracy of ANN result when compared with experimental results.

Adj. R-Square values for the above graphs are as follows:

1. Wear – 0.94801.
2. Coefficient of friction – 0.86097.
3. Frictional force – 0.97377 and pin temperature – 0.81565

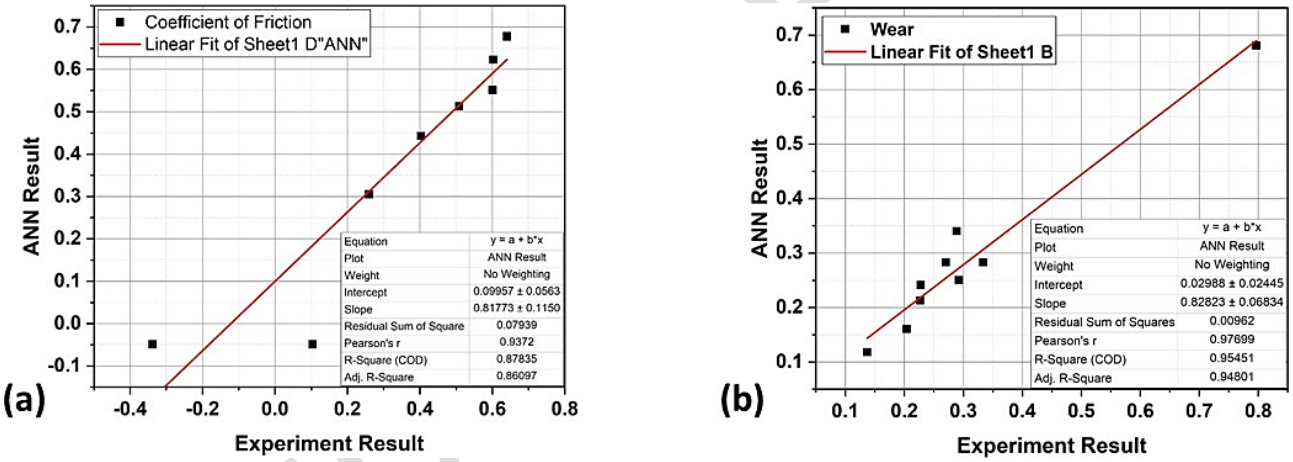

Fig. 13. ANN result v/s Experiment result for wear, ANN result v/s Experiment result for Coefficient of Friction.

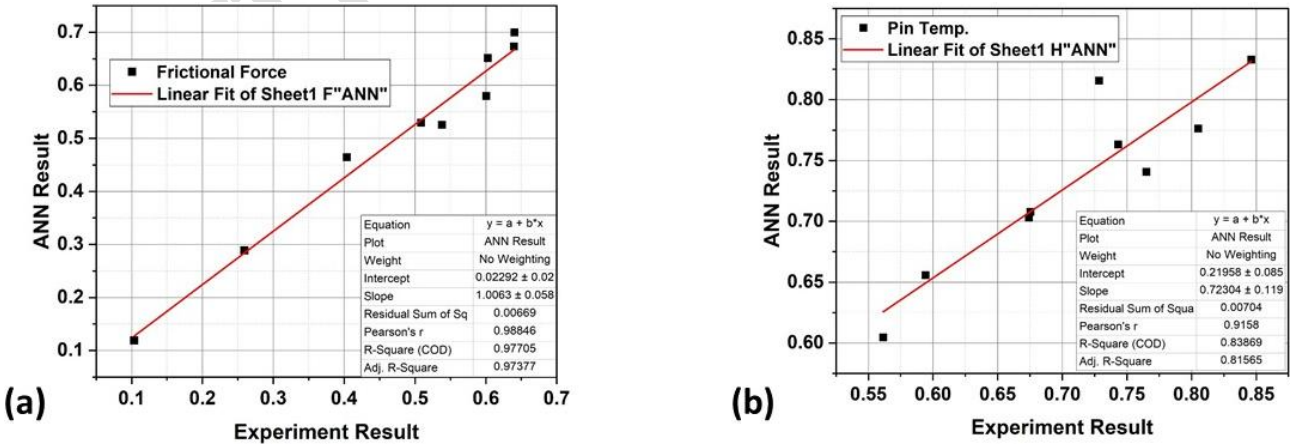

Fig. 14. ANN result v/s Experiment result for Frictional force, ANN result v/s Experiment result for Pin temperature.

5. HARDNESS

Table 4 shows the variation of hardness, as samples printed at a higher NT tend to have a slightly higher Shore D hardness (e.g., Sample 9 with a hardness of 78), which may be due to better material flow and layer adhesion at this elevated temperature. LH is a critical parameter in FDM because it directly influences interlayer bonding, surface finish, and mechanical performance. In the present study, LH values of 0.15 mm, 0.18 mm, and 0.21 mm show a clear effect on surface smoothness and hardness. Smaller LH improve layer-to-layer contact and reduce void formation, resulting in better structural integrity and smoother surfaces, although they increase printing time. is evident in 0.15 mm LH samples, which demonstrate comparatively higher Shore D hardness values due to improved material consolidation. ID also plays a significant role in determining hardness.

Table 4. Hardness result of 3D printed PLA samples.

Sample No.	Nozzle Temperature (NT) in °C	Layer height (LH) in mm	Bed temperature (BT) in °C	Infill density (ID) in %	Shore D Hardness
1	200	0.15	70	50	70
2	200	0.18	75	70	77
3	200	0.21	80	90	73
4	210	0.15	75	90	78
5	210	0.18	80	50	74
6	210	0.21	70	70	74
7	220	0.15	80	70	72
8	220	0.18	70	90	75
9	220	0.21	75	50	78

Keeping high value of ID during 3D printing reduces porosity in greater extent. In case of Sample 3, which has 90% ID exhibited a Shore D hardness of 73, confirming that denser internal geometry enhances stiffness and resistance to indentation. However, hardness is not only governed by infill; NT and LH interactively influence the polymer diffusion and bonding strength. NT affects melt flow and interlayer adhesion which also affects the harness. Sample 4, printed at 210°C NT with 0.15 mm LH and 75°C BT, achieved the highest Shore D hardness of 78, indicating the improved polymer chain mobility and bonding. BT between 70–80°C enhances adhesion, reduces residual stress, and minimizes warping, thereby contributing to improved mechanical properties.

6 . SCANNING ELECTRON MICROSCOPY

Scanning electron microscope (SEM) images for Sample 1 and Sample 8 are presented in Fig. 15 and Fig 16 respectively. These images significantly highlighting the disparities in their worn surface characteristics. Sample 1 reveals a relatively smooth and less damaged surface morphology, with shallow grooves and minimal crack propagation, suggesting mild wear, predominantly governed by micro-abrasion. In contrast, Sample 8 displays severe surface degradation characterized by deep ploughing marks, delamination, and accumulated wear debris, indicating the combination of abrasive and fatigue wear mechanisms.

Presence of fragmented material and crack initiation sited along the layer boundaries further implies weaker interlayer adhesion, contributing to fatigue-induced surface failure. While adhesive wear was not prominently observed, localized material transfer in certain regions of Sample 8 suggests a minor contribution from adhesive interactions. These qualitative observations from SEM micrographs substantiate the quantitative tribological data, wherein Sample 1 exhibited lower mass loss, coefficient of friction (COF), and frictional force compared to Sample 8. Such correlation reinforces the importance of microstructural examination in complementing numerical wear assessment. Furthermore, SEM provides critical insight into microstructural attributes such as inter-layer fusion, void distribution, and surface continuity—all these features play pivotal roles in determining mechanical performance indicators like Shore D hardness. A combined quantitative and qualitative evaluation of wear behavior offers a

Article in Press

holistic understanding of how variations in processing parameters affect the structural integrity and tribological performance of 3D printed components. The morphology of the wear debris observed in the SEM analysis further elucidates the prevailing wear mechanisms.

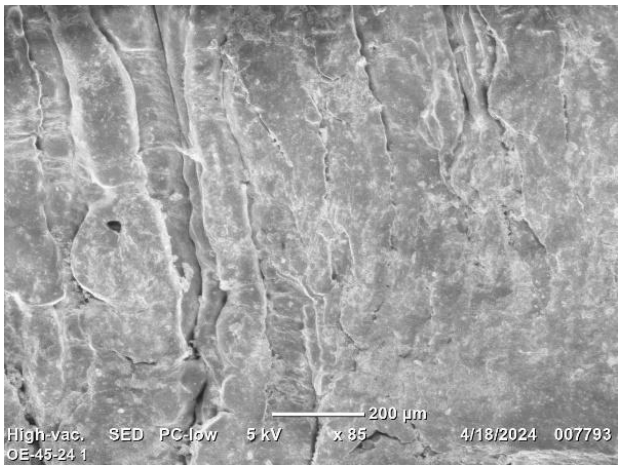

Fig. 15. Sample 1 SEM micrograph.

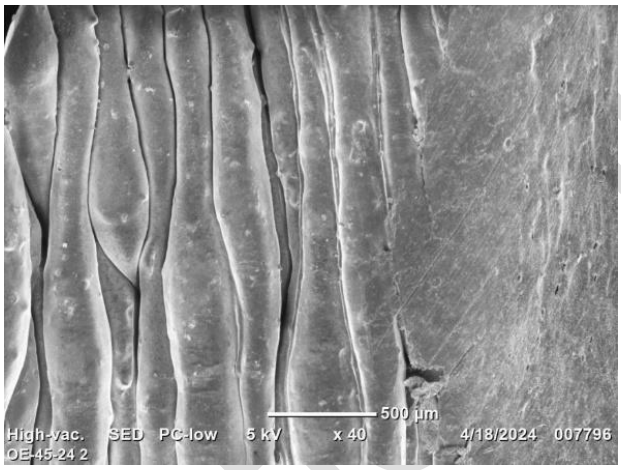

Fig. 16. Sample 8 SEM micrograph.

SEM images of Sample 8 as shown in Fig 16, illustrate that the wear debris predominantly consists of irregular, angular particles with sharp edges, characteristic of brittle fracture and abrasive wear. This indicates that material removal occurred through micro-cutting and fragmentation, likely exacerbated by poor inter-layer bonding and localized stress concentration.

In contrast, Sample 1 produced finer and more rounded debris, suggesting a high ductile wear with limited material removal. Additionally, traces of smeared material on the wear tracks of Sample 8 suggest localized material transfer and adhesion, albeit to a lesser extent, potentially contributing to an increase in frictional resistance during sliding.

The classification of surface damage based on SEM features reveals that Sample 8 underwent a combination of two-body abrasive wear, fatigue-induced crack propagation, and minor adhesive interactions. Meanwhile, the comparatively undamaged morphology of Sample 1 points to a predominantly mild abrasive regime with minimal fatigue involvement. These insights into debris morphology and surface degradation modes offer a more nuanced understanding of the complex tribological behavior influenced by the 3D printing process parameters.

7. CONCLUSIONS

In the present study, the tribological behavior of 3D-printed PLA material was investigated. The samples were prepared by varying the NT, LH, BT, and ID. These samples were subjected to pin-on-disc testing with constant speed, sliding distance, and load conditions.

The following conclusions were drawn from the study:

- Wear behavior: Sample 1 (NT: 200°C, LH: 0.15 mm, BT: 70 °C, ID: 50%) exhibited the lowest wear, while Sample 8 (NT: 220°C, LH: 0.21 mm, BT: 75°C, ID: 50%) showed the highest wear. This variation in wear behavior is attributed to the hardness values. Sample 1 with a lower hardness of 70 Shore D, while Sample 8 with a higher hardness value of 75 Shore D.
- Hardness variation: The hardness of the 3D-printed PLA samples ranged from 70 to 78 Shore D.
- Coefficient of friction: The coefficient of friction increased over time, varying from 0.1 to 0.5.
- Frictional force: Frictional force also increased with time, ranging from 0.5 to 2.5 N.
- Pin temperature: As the testing time increased, the pin temperature also increased for all the samples, temperatures ranging from room temperature up to 37°C.

These findings contribute to understanding the tribological performance of 3D-printed PLA under varying printing conditions and provide insights into optimizing its use for low-stress tribological applications.

Article in Press

Future scope

In this study, tribological parameters such as load, sliding speed, and track radius were kept constant to limit the scope and focus on the influence of 3D printing process parameters on the tribological behavior of PLA. Future work can explore the influence of varying tribological parameters—such as different loads, sliding speeds, and lubrication conditions—on the coefficient of friction, wear rate, and surface degradation. Studying the interaction between process parameters and tribological test conditions will provide a more comprehensive understanding of material performance and guide the optimization of 3D-printed components for real-world applications.

This study provides a foundational understanding of how 3D printing parameters affect the tribological performance of PLA components. Future research could expand by incorporating composite filaments, such as PLA reinforced with carbon fiber, graphene, or natural fibers, to enhance wear resistance and mechanical properties. Additionally, multi-material printing and surface treatments could be explored to reduce friction and improve durability.

Acknowledgement

The authors wish to sincerely acknowledge the financial support from the Science and Engineering Research Board - Department of Science and Technology (EEQ/2021/000763), New Delhi, Government of India and IDEA2PoC Grant Scheme (Elevate-Unnati 2021) of Karnataka Startup Policy, KITS, Dept. of Electronics, IT, BT and S&T Govt. of Karnataka.

REFERENCES

[1] M. Batista, I. Del Sol, Á. Gómez-Parra, and J. M. Vazquez-Martinez, "Tribological performance of additive manufactured PLA-based parts," *Polymers*, vol. 16, no. 17, p. 2529, Sep. 2024, doi: 10.3390/polym16172529.

[2] G. Macovei and V. Paleu, "A review on tribological behaviour of 3D printed mechanical components," *Buletinul Institutului Politehnic Din Iaşi. Secţia Construcţii De Maşini/Buletinul Institutului Politehnic Din Iaşi, Secţia Construcţii De Maşini*, vol. 68, no. 3, pp. 41–56, Sep. 2022, doi: 10.2478/bipcm-2022-0024.

[3] R. Roy and A. Mukhopadhyay, "Tribological studies of 3D printed ABS and PLA plastic parts," *Materials Today Proceedings*, vol. 41, pp. 856–862, Oct. 2021, doi: 10.1016/j.matpr.2020.09.235.

[4] M. Somireddy, C. Singh, and A. Czekanski, "Analysis of the material behavior of 3D printed laminates via FFF," *Experimental Mechanics*, vol. 59, no. 6, pp. 871–881, Apr. 2019, doi: 10.1007/s11340-019-00511-5.

[5] E. R. R. Ghomi *et al.*, "The life cycle assessment for Polylactic Acid (PLA) to make it a Low-Carbon material," *Polymers*, vol. 13, no. 11, p. 1854, Jun. 2021, doi: 10.3390/polym13111854.

[6] M. Hanon and L. Zsidai, "Comprehending the role of process parameters and filament color on the structure and tribological performance of 3D printed PLA," *Journal of Materials Research and Technology*, vol. 15, pp. 647–660, Aug. 2021, doi: 10.1016/j.jmrt.2021.08.061.

[7] A. P. V. Puerta, M. B. Ponce, S. R. F. Vidal, and F. G. Mata, "Post-Processing Of Pla Parts After Additive Manufacturing By Fdm Technology," *Dyna*, vol. 93, no. 1, pp. 625–629, Oct. 2018, doi: 10.6036/8859.

[8] A. A. Fote, A. H. Wildvank, and R. A. Slade, "Coefficient of friction of PTFE-impregnated porous bronze versus temperature," *Wear*, vol. 47, no. 2, pp. 255–261, Apr. 1978, doi: 10.1016/0043-1648(78)90156-4.

[9] R. Muntean, S. Ambruş, N. A. Sîrbu, and I. D. Uţu, "Tribological properties of different 3D printed PLA filaments," *Nano Hybrids and Composites*, vol. 36, pp. 103–111, Jun. 2022, doi: 10.4028/p-8k2v92.

[10] S. R. Kishore, A. Mathew, A. T. Tomy, M. Sugavaneswaran, and A. J. Rajan, "Design and development of hot vapour polishing system and optimization of it's process parameters for FDM printed parts," *Tribology in Industry*, vol. 44, no. 4, pp. 551–567, Dec. 2022, doi: 10.24874/ti.1305.05.22.09.

[11] M. A. Ramadan, H. A. Sabour, and E. EL-Shenawy, "Tribological properties of 3D printed polymers: PCL, ABS, PLA and co-polyester," *Tribology in Industry*, vol. 45, no. 1, pp. 161–167, Mar. 2023, doi: 10.24874/ti.1410.11.22.02.

[12] M. Hanon, Y. Alshammas, and L. Zsidai, "Effect of print orientation and bronze existence on tribological and mechanical properties of 3D-printed bronze/PLA composite," *The International Journal of Advanced Manufacturing Technology*, vol. 108, no. 1–2, pp. 553–570, May 2020, doi: 10.1007/s00170-020-05391-x.

[13] N. Stoimenov, M. Kandeva, M. Zagorski, and P. Panev, "Static and kinetic friction of 3D printed polymers and composites," *Tribology in Industry*, vol. 46, no. 1, pp. 97–106, Mar. 2024, doi: 10.24874/ti.1546.08.23.10.

Article in Press

[14] S. V. Gubbewad and A. Raichur, "Evaluation of Wear Model Equations Through Analysis of Experimental Wear Data of Materials from Literature," *Tribology in Industry*, vol. 46, no. 2, pp. 260–269, Jun. 2024, doi: 10.24874/ti.1555.09.23.11.

[15] F. O. Kolawole, A. T. Ayeni, S. K. Kolawole, O. S. Kolade, and A. F. Owa, "Statistical models for predicting wear and friction coefficient of valve tappet using ANOVA," *Tribology in Industry*, vol. 46, no. 2, pp. 210–216, Jun. 2024, doi: 10.24874/ti.1517.07.23.09.

[16] M. Grasso, L. Azzouz, P. Ruiz-Hincapie, M. Zarrelli, and G. Ren, "Effect of temperature on the mechanical properties of 3D-printed PLA tensile specimens," *Rapid Prototyping Journal*, vol. 24, no. 8, pp. 1337–1346, Oct. 2018, doi: 10.1108/rpj-04-2017-0055.

[17] S. Farah, D. G. Anderson, and R. Langer, "Physical and mechanical properties of PLA, and their functions in widespread applications — A comprehensive review," *Advanced Drug Delivery Reviews*, vol. 107, pp. 367–392, Jun. 2016, doi: 10.1016/j.addr.2016.06.012.

[18] S. Perepelkina, P. Kovalenko, R. Pechenko, and K. Makhmudova, "Investigation of Friction Coefficient of Various Polymers Used in Rapid Prototyping Technologies with Different Settings of 3D Printing," *Tribology in Industry*, vol. 39, no. 4, pp. 519–526, Dec. 2017, doi: 10.24874/ti.2017.39.04.11.

[19] A. E. Magri, K. E. Mabrouk, S. Vaudreuil, and M. E. Touhami, "Mechanical properties of CF-reinforced PLA parts manufactured by fused deposition modeling," *Journal of Thermoplastic Composite Materials*, vol. 34, no. 5, pp. 581–595, May 2019, doi: 10.1177/0892705719847244.

[20] M. Behzadnasab, A. A. Yousefi, D. Ebrahimibagha, and F. Nasiri, "Effects of processing conditions on mechanical properties of PLA printed parts," *Rapid Prototyping Journal*, vol. 26, no. 2, pp. 381–389, Oct. 2019, doi: 10.1108/rpj-02-2019-0048.

[21] J. S. Bergström and D. Hayman, "An overview of mechanical properties and material modeling of polylactide (PLA) for medical applications,"*Annals of Biomedical Engineering*, vol. 44, no. 2, pp. 330–340, Sep. 2015, doi: 10.1007/s10439-015-1455-8.

[22] J.-H. Park, S.-H. Kim, J.-Y. Park, S.-G. Kim, Y.-J. Lee, and J.-H. Kim, "Prediction of microstructure and mechanical properties of ultrasonically treated PLA materials using convolutional neural networks," *International Journal of Precision Engineering and Manufacturing*, vol. 26, no. 1, pp. 239–248, Jul. 2024, doi: 10.1007/s12541-024-01081-w.

[23] Y. Guo, Z. Guo, and Z. Yin, "Evaluating the mechanical and tribological properties of 3D printed PLA/n-HA/PA66 composite," *Journal of Applied Polymer Science*, vol. 142, no. 16, Jan. 2025, doi: 10.1002/app.56771.

[24] P. Arunkumar, D. Balaji, N. Radhika, L. Rajeshkumar, Sanjay, and S. Siengchin, "Effect of infill pattern on mechanical properties of 3D printed PLA-Zn composites for drone frame structures: A topology optimization integrated application study," *Results in Engineering*, vol. 25, p. 104107, Jan. 2025. doi: 10.1016/j.rineng.2025.104107.

[25] L. Calabrese et al., "Optimization of deposition temperature and gyroid infill to improve flexural performance of PLA and PLA–flax fiber composite sandwich structures," *Journal of Manufacturing and Materials Processing*, vol. 9, no. 2, p. 31, Jan. 2025, doi: 10.3390/jmmp9020031.

[26] P. Singhal, P. Katiyar, U. Ramachandran, S. Davuluri, and R. Sujithra, "Mode-I and mode-II fracture toughness investigation on FDM-printed PLA/CF-PLA laminate composite," *Journal of Mechanical Science and Technology*, vol. 39, no. 1, pp. 129–136, Jan. 2025, doi: 10.1007/s12206-024-1212-8.

[27] R. C. Zapata, D. P. Ramírez, J. J. C. Pérez, H. D. Rosales, B. B. Díaz, and J. a. A. Adame, "Mechanical and thermal evaluation of PLA/PLA-g-MA/MCC composites via reactive extrusion," *MRS Advances*, vol. 8, no. 23, pp. 1325–1329, Nov. 2023, doi: 10.1557/s43580-023-00683-2.

[28] R. Kumar and R. Singh, "On 3D printing of architected PLA-PLA Nanofiber-Based biomedical scaffolds," *National Academy Science Letters*, vol. 46, no. 5, pp. 391–395, May 2023, doi: 10.1007/s40009-023-01261-8.

[29] E. Vălean, P. Foti, S. M. J. Razavi, F. Berto, and L. Marşavina, "Static and fatigue behavior of 3D printed PLA and PLA reinforced with short carbon fibers," *Journal of Mechanical Science and Technology*, vol. 37, no. 11, pp. 5555–5559, Oct. 2023, doi: 10.1007/s12206-023-2307-3.

[30] K. Goryl, M. Pollák, M. Kočiško, and M. Korol, "Comparison of PLA and PLA carbon fiber materials on tensile test," in *Lecture notes in mechanical engineering*, 2024, pp. 73–82. doi: 10.1007/978-3-031-56463-5_6.

[31] Y. Elmoghazy, E. M. O. Abuelgasim, S. A. Osman, Y. R. H. Afaneh, O. M. A. Eissa, and B. Safaei, "Effective mechanical properties evaluation of unidirectional and bidirectional composites using virtual domain approach at microscale," *Archives of Advanced Engineering Science*, vol. 1, no. 1, pp. 27–37, Oct. 2023, doi: 10.47852/bonviewaaes32021723.

[32] O. Shekoofa, J. Wang, and D. Li, "Fabrication of N-Type nanocrystalline silicon Thin-Film by magnetron sputtering and antimony induced crystallization," *Archives of Advanced Engineering Science*, vol. 2, no. 2, pp. 71–78, May 2023, doi: 10.47852/bonviewaaes32021040.

Article in Press

[33] K. Dey, K. Kalita, and S. Chakraborty, "Prediction performance analysis of neural network models for an electrical discharge turning process," *International Journal on Interactive Design and Manufacturing (IJIDeM)*, vol. 17, no. 2, pp. 827–845, Aug. 2022, doi: 10.1007/s12008-022-01003-y.

[34] B. Rachaiah, J. T. Puttaswamy, S. B. Nagaraju, and D. H. Vedavathi, "Investigation on the wear characteristics of 3D printed graphene-reinforced PLA composites," *Discover Materials*, vol. 4, no. 1, Nov. 2024, doi: 10.1007/s43939-024-00152-z.

[35] J. Bustillos, D. Montero, P. Nautiyal, A. Loganathan, B. Boesl, and A. Agarwal, "Integration of graphene in poly(lactic) acid by 3D printing to develop creep and wear-resistant hierarchical nanocomposites," *Polymer Composites*, vol. 39, no. 11, pp. 3877–3888, May 2017, doi: 10.1002/pc.24422.

[36] J. Sun and S. Du, "Application of graphene derivatives and their nanocomposites in tribology and lubrication: A review," *RSC Advances*, vol. 9, no. 69, pp. 40642–40661, Jan. 2019, doi: 10.1039/c9ra05679c.

[37] S. R. Laraba et al., "Enhancing the tribological performance of PLA-based biocomposites reinforced with graphene oxide," *Journal of the Mechanical Behavior of Biomedical Materials/Journal of Mechanical Behavior of Biomedical Materials*, vol. 148, p. 106224, Nov. 2023, doi: 10.1016/j.jmbbm.2023.106224.

[38] J. Santo, V. Pradhik, S. Kalakoti, P. Saravanan, and P. K. Penumakala, "Effect of composite processing technique on tribological properties of 3D printed PLA - graphene composites," *Tribology International*, vol. 198, p. 109895, Jun. 2024, doi: 10.1016/j.triboint.2024.109895.

[39] T. Batakliev, "Tribological investigation of PLA-based nanocomposites by scratch and wear experiments," *Journal of Theoretical and Applied Mechanics*, vol. 50, no. 2, May 2020, doi: 10.7546/jtam.50.20.02.01.

[40] A. A. Abir and B. Trindade, "A comparative study of different poly (Lactic acid) Bio-Composites produced by mechanical alloying and casting for tribological applications," *Materials*, vol. 16, no. 4, p. 1608, Feb. 2023, doi: 10.3390/ma16041608.

[41] S. Kumar, N. Sharma, and K. K. Singh, "Artificial Neural Network technique to assess tribological performance of GFRP composites incorporated with graphene nano-platelets," *Tribology International*, vol. 179, p. 108194, Dec. 2022, doi: 10.1016/j.triboint.2022.108194.

[42] J. Walker *et al.*, "Application of tribological artificial neural networks in machine elements," *Tribology Letters*, vol. 71, no. 1, Nov. 2022, doi: 10.1007/s11249-022-01673-5.

[43] N. Yin, P. Yang, S. Liu, S. Pan, and Z. Zhang, "AI for tribology: Present and future," *Friction*, vol. 12, no. 6, pp. 1060–1097, Mar. 2024, doi: 10.1007/s40544-024-0879-2.

Article in Press